JTE HCMUTE
ISSN: 2615-9740

JOURNAL OF TECHNICAL EDUCATION SCIENCE
Ho Chi Minh City University of Technology and Education
Website: https://jte.edu.vn
Email: jte@hcmute.edu.vn

A Comprehensive Survey on Linear Quadratic Regulator Control for Unicycle Robots: Experimental Insights

Thi Ai Van Nguyen[1], Dinh Hau Vu[1*], Van Thuyen Ngo[1], Tran Minh Nguyet Nguyen[1], Vi Do Tran[2], Dinh Phu Nguyen[1], Van Dong Hai Nguyen[1], Minh Tai Vo[2], Binh Hau Nguyen[2], Minh Tam Nguyen[1]

[1]*Ho Chi Minh City University of Technology and Education, Vietnam*
[2]*Posts and Telecommunications Institute of Technology (PTIT), Ho Chi Minh City, Vietnam*

[*]Corresponding author. *Email: 20151362@student.hcmute.edu.vn*

ARTICLE INFO

Received: 06/09/2024
Revised: 03/11/2024
Accepted: 24/12/2024
Published:

KEYWORDS

Unicycle;
LQR control;
PID control;
Balance control;
Self-balance.

ABSTRACT

This paper presents an experimental study on the application of Linear Quadratic Regulator (LQR) control for stabilizing a unicycle robot, or one-wheel mobile robot, a prominent example in the unicycle-type mobile robot group. Although inherently unstable, it offers several advantages over multi-wheeled, statically stable robots, such as requiring less space due to its single point of ground contact. The unicycle robot features two axes representing the two models used for analysis: the roll axis, modeled as an inverted pendulum controlled by the wheel, and the pitch axis, modeled as a reaction wheel inverted pendulum controlled by a reaction disk. LQR technique is a great method for developing a controller for nonlinear systems. Our approach involves designing, implementing, and evaluating LQR controllers with varied weighting matrices to assess their impact on system performance. Case studies are conducted by adjusting the weighting matrices of the LQR controllers and comparing each configuration with the initial LQR. Experimental results provide insights into the effectiveness of LQR for achieving robust control of unicycle robots.

Doi: https://doi.org/10.54644/jte.2025.1649

1. Introduction

Unicycle was first introduced in [1], where the study provided mathematical equations and examined controllability of the model. In a subsequent study [2], the design of a unicycle robot was based on the concept of a human riding a unicycle. That paper presented mathematical equations to balance the robot without using a controller, but the model remained unstable and overly complex. Despite these issues, it inspired future developments: Honda created the UX-3 as a personal vehicle, and Murata Manufacturing developed the Murata Girl. In [3], new dynamic equations were introduced, dividing the robot into two parts: the upper reaction wheel pendulum and the lower inverted pendulum, which were decoupled. This research employed intelligent algorithms such as fuzzy logic for each dynamic part, though high-speed movement led to increased balancing time and adaptability. Dynamic control for roll and pitch axes of the unicycle was explored in [4]-[5], where robust control was used for rolling and linear control for pitching, although there was still some chattering in output, even when a signum function was implemented to reduce it. A new single-wheel model with active omnidirectional wheels was introduced, but it also had mechanical limitations [6].

To address the balancing time issues in [3] and the chattering in [4]-[5], we applied a linear controller to this model. This paper in developed from the kinematic analysis and linear controller design in [10], providing experimental evaluations that compare with the theoretical framework for the unicycle robot. A Linear Quadratic Regulator (LQR) was designed for the roll and pitch axes, focusing on finding suitable values in the matrices. The calibration of these values was incorporated and demonstrated through experiments, showing that the linear controller is effective for this model. Additionally, the calibration process was shown to align with the theoretical framework [7]-[8].

JTE
HCMUTE
ISSN: 2615-9740

JOURNAL OF TECHNICAL EDUCATION SCIENCE
Ho Chi Minh City University of Technology and Education
Website: https://jte.edu.vn
Email: jte@hcmute.edu.vn

2. Dynamic models

In this section, we examine the operation of the unicycle robot. The model is divided into two independent bodies for the pitch and roll axes: an inverted pendulum for the pitch axis and a reaction wheel-balanced inverted pendulum for the roll axis. The dynamic models for the unicycle robot's roll and pitch axes were derived using the Lagrange method. Figure 1 illustrates the developed unicycle robot, which consists of three main components: a rotating disk, the robot body, and a rotating wheel, with their respective masses denoted as m_D, m_B, m_W.

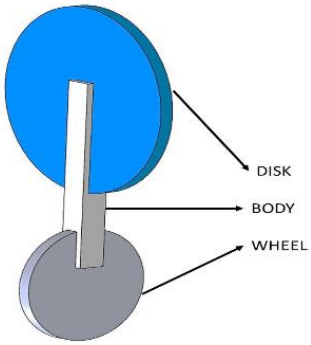

Figure 1. *A basic representation of the unicycle robot model.*

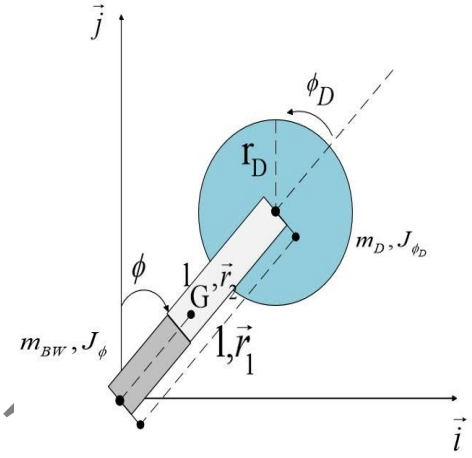

Figure 2. *Model of the unicycle robot for roll axis.*

2.1. Dynamic model for the roll axis

Roll axis dynamics are derived from reaction wheel balance inverted pendulum, which consists of two primary components: a disk and a body compound wheel, collectively referred to as the bottom body. Figure 2 illustrates the robot's axes used for calculating the dynamic roll. The symbols l and l_G represent the distances from the ground to the center of the disk and the center of gravity of the bottom body, respectively. r_D and ϕ_D denote the disk's radius and rotation angle, while ϕ signifies the rotation angle in the roll direction of the robot. The masses of the bottom body, the robot body, and the disk are represented as m_{BW}, m_B, m_D respectively. Two position vectors $\vec{r}_1, \vec{r}_2$ are defined to compute the Lagrangian for robot: one vector extends from the coordinate origin to center of the disk, and other extends from the coordinate origin to the center of the bottom body.

$$\vec{r_1} = l_G \sin(\phi)\vec{i} + l_G \cos(\phi)\vec{j}; \vec{r_2} = l\sin(\phi)\vec{i} + l\cos(\phi)\vec{j} \quad (1)$$

From Section 2.1 of [10], we obtain the following formula:

$$\alpha v_R = (J_\phi + l_G^2 m + l^2 m_D)\ddot{\phi} - g(l_G m + l m_D)\phi - \beta(\dot{\phi} - \dot{\phi}_D); -\alpha v_R = J_{\phi_D}(\ddot{\phi}_D + \phi) + \beta(\dot{\phi} - \dot{\phi}_D) \quad (2)$$

where $\alpha = nKt / R_m, \beta = \alpha + f_m$

2.2. Dynamic model for the pitch axis

Dynamics of pitch axis are calculated based on an inverted pendulum model, which consists of two main components: wheel and a compound disk representing body, referred to as the upper body. Fig. 3 illustrates robot's axes used to calculate pitch dynamics. L represents distance from center of the wheel to center of upper body. R_W is radius of wheel, while θ_W and θ represent rotational angles of wheel and pitch axis dynamic model, respectively. m_W and m_{BD} denote masses of wheel and upper body.

JTE
HCMUTE
ISSN: 2615-9740

JOURNAL OF TECHNICAL EDUCATION SCIENCE
Ho Chi Minh City University of Technology and Education
Website: https://jte.edu.vn
Email: jte@hcmute.edu.vn

Two position vectors, $\vec{r}_1, \vec{r}_2$, are defined to calculate Lagrangian for robot, representing vectors from coordinate origin to center of wheel and center of upper body.

$$\begin{aligned}\vec{r_1} &= R_W\theta_W\vec{i} + R_W\vec{j} \\ \vec{r_2} &= (R_W\phi + L_C\sin\theta)\vec{i} + (R_W + L_C\cos\theta)\vec{j}\end{aligned} \tag{3}$$

From Section 2.2 of [10], we obtain the following formula:

$$\begin{aligned}\alpha v_P &= \left(J_{\theta_W} + J_m n^2 + (m_W + m_{BD})R^2{}_W\right)\ddot{\theta}_W + \left(L_C m_{BD} R_W - J_m n^2\right)\ddot{\theta} + \beta\dot{\theta}_W - \beta\dot{\theta} \\ -\alpha v_P &= (L_C m_{BD} R_W - J_m n^2)\ddot{\theta}_W - \beta\dot{\theta}_W + \beta\dot{\theta} - gL_C m_{BD}\theta + \left(J_\psi + L_C{}^2 m_{BD} + J_m n^2\right)\ddot{\theta}\end{aligned} \tag{4}$$

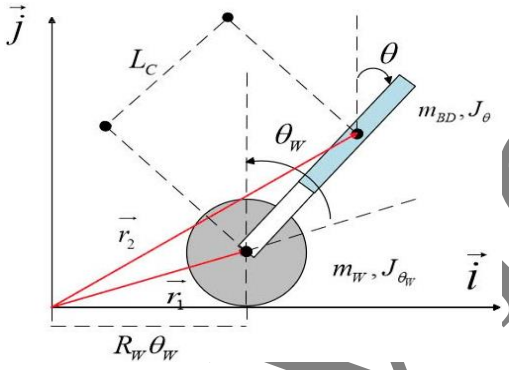

Figure 3. *Model of unicycle for pitch axis*

3. Design of LQR

3.1. LQR for Roll axis

From Section 4.1 of [10], we obtain matrices $\mathbf{Q}, \mathbf{R}$ as

$$\mathbf{Q} = \begin{bmatrix} Q_1 & 0 & 0 & 0 \\ 0 & Q_2 & 0 & 0 \\ 0 & 0 & Q_3 & 0 \\ 0 & 0 & 0 & Q_4 \end{bmatrix}; \mathbf{R} = [R_1] \tag{5}$$

Coefficients Q_1, Q_2, Q_3, Q_4 indicate importance assigned to state variables x_1, x_2, x_4, x_5. If one of these coefficients is increased, corresponding variable will be more responsive than the others. However, this adjustment could potentially stabilize system while causing robot losing balance. Therefore, careful selection of $\mathbf{Q}$ is essential. $\mathbf{R}$ represents the priority given to the input v_R

The values of matrices $\mathbf{Q}, \mathbf{R}$ were chosen as follows:

$$Q_1=350;\ Q_2=10;\ Q_3=100;\ Q_4=10;\ R=R_1=1 \tag{6}$$

The optimal gain can be determined [8], [9] as follows:

$$K = \begin{bmatrix} -34.9638 & -4.0849 & -10.0000 & -8.1591 \end{bmatrix} \tag{7}$$

The control input is defined as:

$$v_R = -Kx \tag{8}$$

where $x = \begin{bmatrix} x_1 & x_2 & x_4 & x_5 \end{bmatrix}^T = \begin{bmatrix} \phi & \dot{\phi} & \phi_D & \dot{\phi}_D \end{bmatrix}^T; e_\phi = \phi - \phi_{ref}; e_{\phi_D} = \phi_D - \phi_{Dref}$

3.2. LQR for Pitch axis

From Section 4.2 of [10], we obtain matrices $\mathbf{Q},\mathbf{R}$ as below:

$$\mathbf{Q}=\begin{bmatrix} Q_5 & 0 & 0 & 0 \\ 0 & Q_6 & 0 & 0 \\ 0 & 0 & Q_7 & 0 \\ 0 & 0 & 0 & Q_8 \end{bmatrix};\mathbf{R}=[R_2] \tag{9}$$

The values of matrices $\mathbf{Q},\mathbf{R}$ were chosen as follows:

$$Q_1=350;\ Q_2=10;\ Q_3=100;\ Q_4=10;\ R=R_2=1 \tag{10}$$

Thence, matrix K is obtained as

$$K=\begin{bmatrix}48.1396 & 10.3124 & 10.0000 & 10.3962\end{bmatrix} \tag{11}$$

The control input is defined as:

$$v_P=-Kx \tag{12}$$

where $x=\begin{bmatrix}x_7 & x_8 & x_{10} & x_{11}\end{bmatrix}^T=\begin{bmatrix}\theta_W & \dot{\theta}_W & \theta & \dot{\theta}\end{bmatrix}^T;e_{\theta_W}=\theta_W-\theta_{W\,ref};e_\theta=\theta-\theta_{ref}$

4. Experiments

4.1. Standard LQR

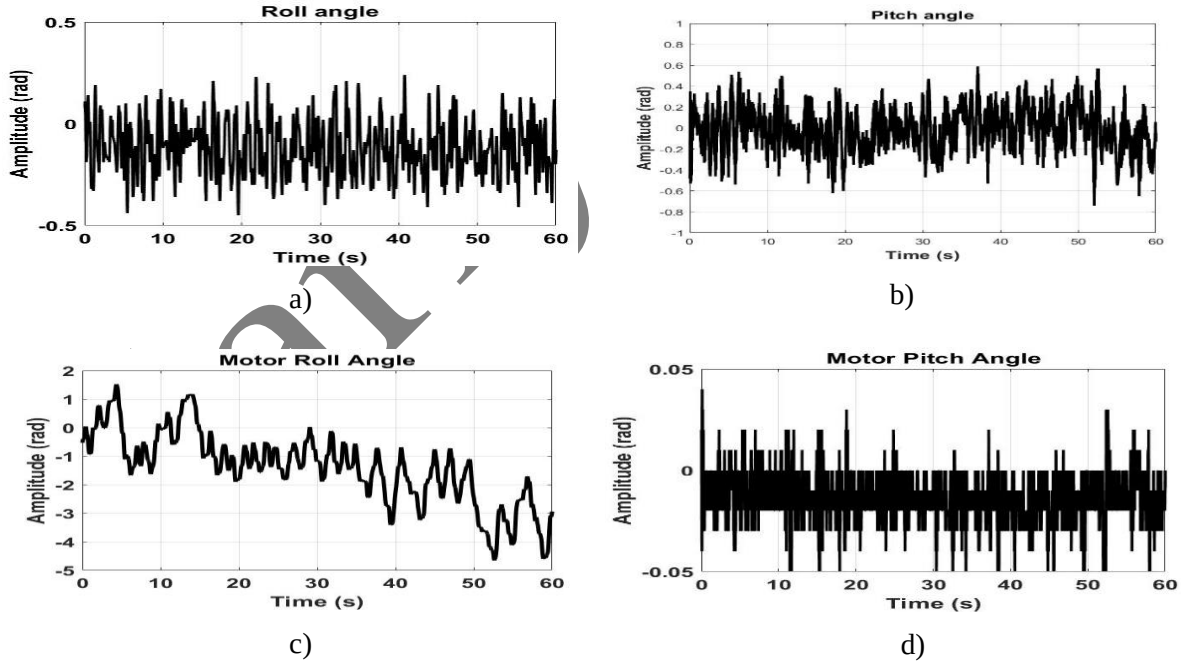

Figure 4. *a) Stable LQR value of Roll axis b) Stable LQR value for Pitch axis c) Output result of the disk motor d) Output result of the wheel motor*

Comment: Observing the data, we can easily see that over the 60-second period, both the roll and pitch angles oscillate around the equilibrium position. The roll motor angle stabilizes at 0 in the first 20s and then gently shifts backward. Meanwhile, the pitch motor angle responds well, keeping the robot in the optimal state.

JTE
HCMUTE
ISSN: 2615-9740

JOURNAL OF TECHNICAL EDUCATION SCIENCE
Ho Chi Minh City University of Technology and Education
Website: https://jte.edu.vn
Email: jte@hcmute.edu.vn

4.2. Modify Q_1 value

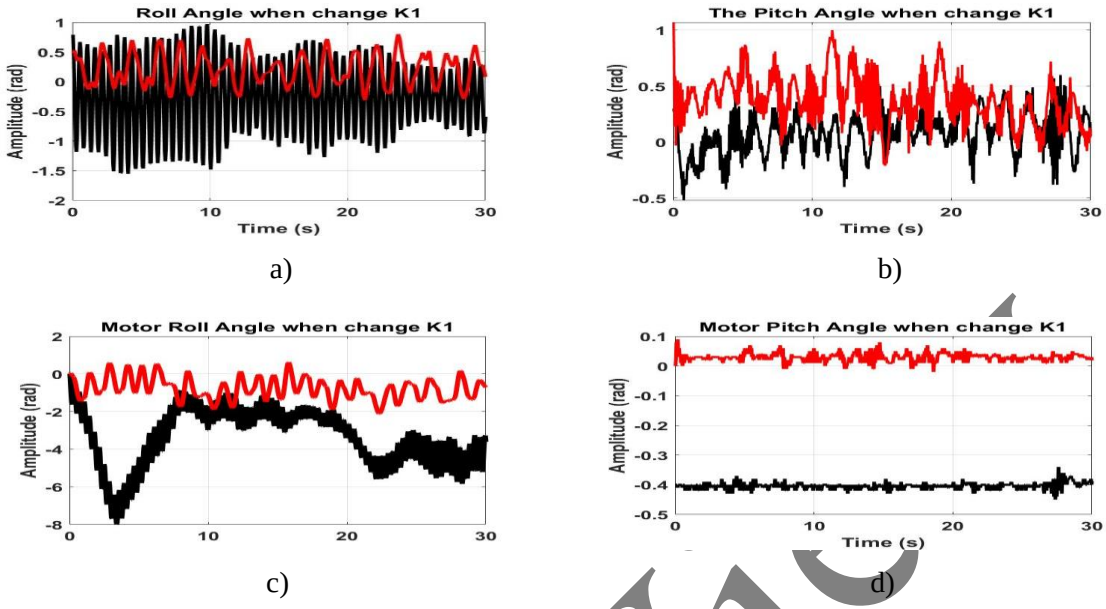

Figure 5. *a) Modify Q_1 value of Roll axis b) Modify Q_1 value for Pitch axis c) Output result of the disk motor d) Output result of the wheel motor (Black line is K1=2.8; Red line is K1=1.2)*

Comment:

When Q_1 increases, figures 5 a-b show the roll angle oscillates around the equilibrium position with a larger amplitude ranging from [-1.5;1] rad and the pitch angle tilts significantly during the first 10s and gradually stabilizes, oscillating within [-0.5;0.5] rad. Additionally, figures 5 c-d illustrate the roll motor angle moves up and down continuously, Meanwhile, the pitch motor angle tilts by 0.4 rad.

When Q_1 decreases, figures 5 a-b prove the control signals for the roll and pitch angles, as well as figures 5 c-d indicate the roll and pitch motor angles, oscillate around 0 with a greater amplitude compared to the standard Q_1 value.

4.3. Modify Q_2 value

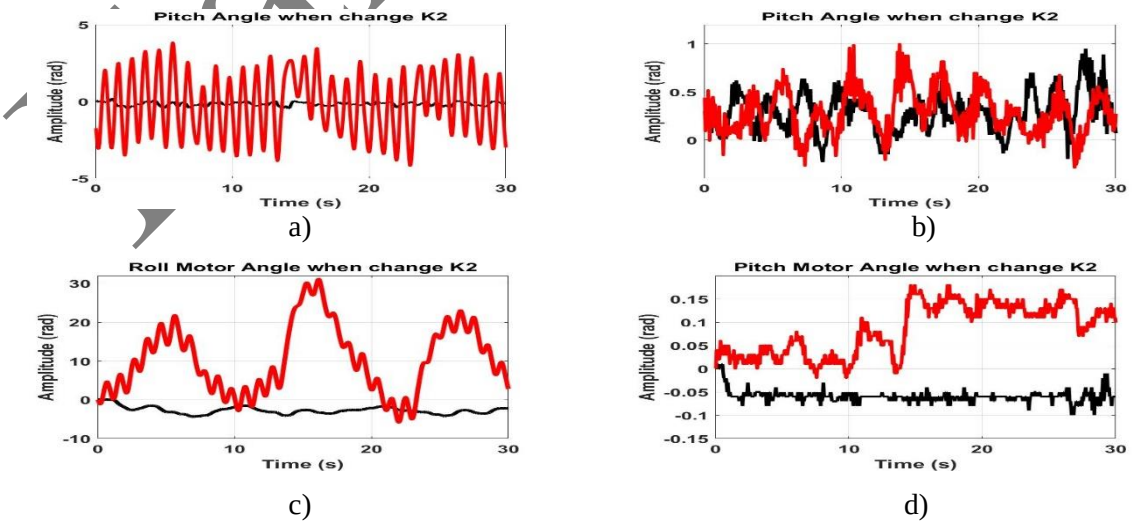

Figure 6. *a) Modify Q_2 value of Roll axis b) Modify Q_2 value for Pitch axis c) Output result of the disk motor d) Output result of the wheel motor (Black line is K2=0.35; Red line is K2=0.2)*

JTE
HCMUTE
ISSN: 2615-9740

JOURNAL OF TECHNICAL EDUCATION SCIENCE
Ho Chi Minh City University of Technology and Education
Website: https://jte.edu.vn
Email: jte@hcmute.edu.vn

Comment:

When Q_2 increases, figures 6 a-b show the roll angle oscillates steadily around the equilibrium position and the pitch angle oscillates around 0 within the range of [-0.2;0.2] rad. Along with that, figures 6 c-d illustrate the roll motor angle gradually moves backward, meanwhile, the pitch motor angle stabilizes at 0 for about 5s and then tilts by 0.05 rad.

When Q_2 decreases, figures 6 a-b prove the roll and pitch angles oscillate around 0 with wider amplitudes ranging from [-4;4] rad and [-0.2;1] rad, respectively. The figures 6 c-d indicate the roll motor angle changes continuously, increasing and decreasing once every 10s within the ranges [0;22], [0;31], [0;23] rad, meanwhile, the pitch motor angle remains stable for the first 20s and then gradually increases to 0.18 rad at the 30s mark, maintaining that tilt.

4.4. Modify Q_3 value

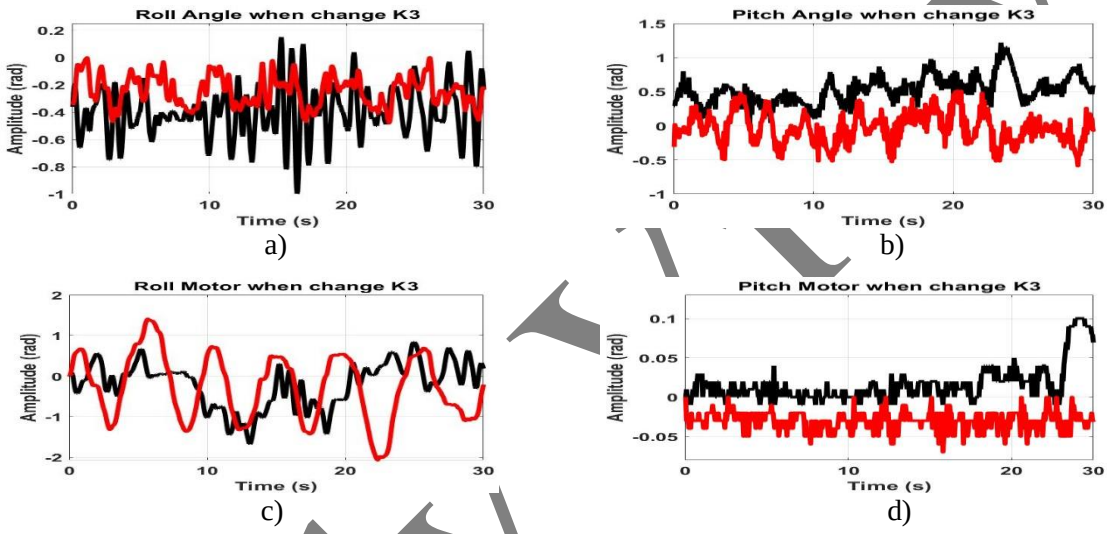

Figure 7. *a) Modify Q_3 value of Roll axis b) Modify Q_3 value for Pitch axis c) Output result of the disk motor d) Output result of the wheel motor (Black line is K3=0.8; Red line is K3=0.3)*

Comment:

When Q_3 increases, figures 7 a-b indicate the roll angle oscillates steadily around -0.5 rad with an amplitude of 0.5 rad, while the pitch angle oscillates around 0.4 rad. Additionally, figures 7 c-d illustrate the roll motor angle stabilizes at 0 during the first 10s, then decreases to -1.5 rad over the next 20s, and gradually increases to 1 rad in the final 20s, meanwhile, the pitch motor angle stabilizes at 0 with a small amplitude of 0.02 rad for the first 25s, then overshoots to 0.12 rad.

When Q_3 decreases, figures 7 a-b show the roll angle oscillates at -0.25 rad and the pitch angle oscillates around 0 within the range of [-0.4;0.4] rad. Figures 7 c-d prove the roll motor angle stabilizes at 0 with an amplitude of about 1.5 rad, meanwhile, the pitch motor angle stabilizes at -0.02 rad.

4.5. Modify Q_4 value

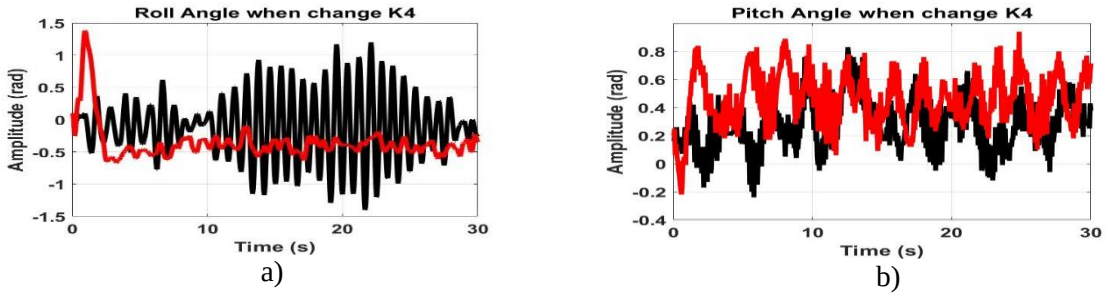

JTE
HCMUTE
ISSN: 2615-9740

JOURNAL OF TECHNICAL EDUCATION SCIENCE
Ho Chi Minh City University of Technology and Education
Website: https://jte.edu.vn
Email: jte@hcmute.edu.vn

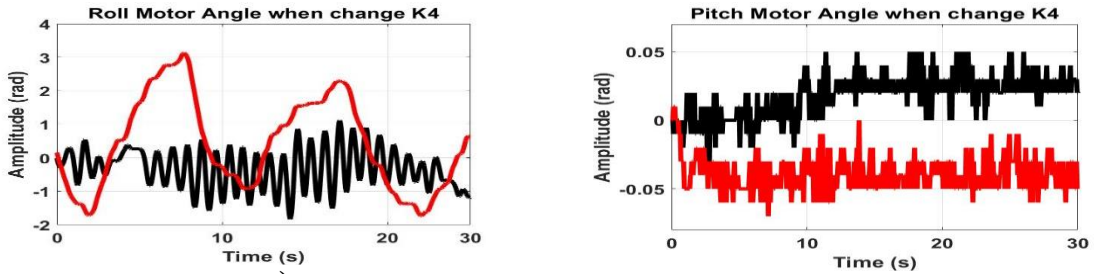

Figure 8. *a) Modify Q_4 value of Roll axis b) Modify Q_4 value for Pitch axis c) Output result of the disk motor d) Output result of the wheel motor (Black line is K4=0.18; Red line is K4=0.1)*

Comment:

When increasing Q_4, figures 8 a-b show that within the first 10s, the roll angle oscillates around the equilibrium position with an amplitude ranging from [-0.6; 0.6] rad and then expands to an amplitude of [-1.4; 1.3] rad, simultaneously, the pitch angle oscillates steadily around 0.4 rad. figures 8 c-d illustrate the roll motor stabilizes at 0 in the first 5s and then gradually stabilizes at -0.5 rad, meanwhile, the pitch motor remains stable at 0 for a longer period, around 15s, and then gradually stabilizes at 0.02 rad.

When decreasing Q_4, figures 8 a-b show the roll angle overshoots to 1.4 rad in the first second, then decreases to -0.5 rad and oscillates around that position, additionally, the pitch angle oscillates around 0.4 rad, showing some deviation compared to when Q_4 is increased, but it does not significantly affect the system. The figures 8 c-d prove the roll motor oscillates with a large amplitude but not excessively, making it difficult for the robot to balance and the pitch motor decreases to -0.04 rad at the 2s and then stabilizes around that point.

4.6. Modify Q_5 value

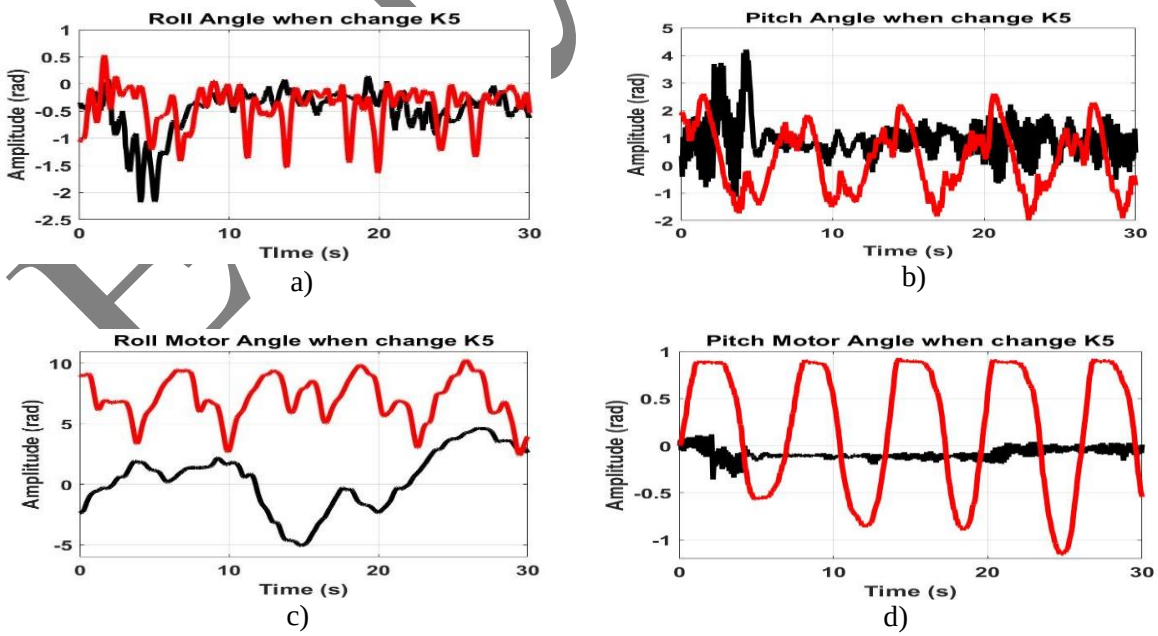

Figure 9. *Modify Q_5 value of Roll axis b) Modify Q_5 value for Pitch axis c) Output result of the disk motor d) Output result of the wheel motor (Black line is K5=0.9; Red line is K5=0.4)*

Comment:

When increasing Q_5, figures 9 a-b show that the roll angle oscillates around the position of -0.25 rad, but between 3-5s, the signal drops to -2.2 rad, simultaneously, during the first 5s, the pitch angle oscillates significantly around 1 rad with an amplitude of 4 rad, and then the amplitude gradually decreases in the later stage. Figures 9 c-d illustrate the roll motor oscillates slightly around the 0 position, meanwhile, the pitch motor oscillates around -0.01 rad with a relatively small amplitude.

When decreasing Q_5, figures 9 a-b indicate the roll angle oscillates around -0.25 rad, but between 2-5s, the signal overshoots to 0.5 rad, however, the pitch angle oscillates with a large amplitude but not frequently. The figures 9 c-d prove the roll and pitch motors do not oscillate much, making it difficult for the system to maintain stable balance.

4.7. Modify Q_6 value

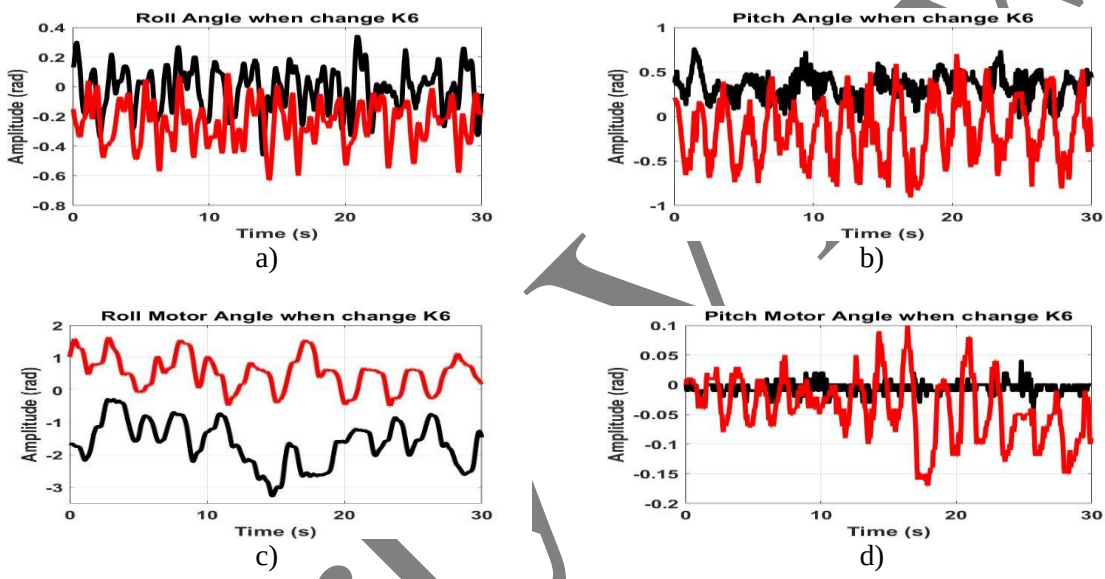

Figure 10. *Modify Q_6 value of Roll axis b) Modify Q_6 value for Pitch axis c) Output result of the disk motor d) Output result of the wheel motor (Black line is K6=1.2; Red line is K6=0.05)*

Comment:

When increasing Q_6, figures 10 a-b show that roll angle oscillates around 0 and pitch angle oscillates around 0.4 rad. Figures 10 c-d illustrate roll motor oscillates slightly around -1.5 rad, meanwhile, pitch motor oscillates steadily around equilibrium position with a relatively small amplitude.

When decreasing Q_6, figures 10 a-b indicate the roll and pitch angles oscillate around -0.2 rad, but the pitch angle oscillates with a larger amplitude compared to the roll angle. Figures 10 a-b prove the roll motor oscillates slightly around 0.5 rad, meanwhile, the pitch motor oscillates steadily around the equilibrium position with an amplitude that gradually increases over time.

4.8. Modify Q_7 value

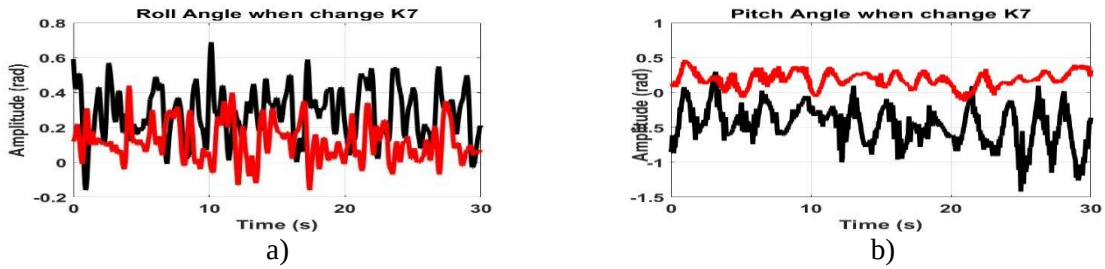

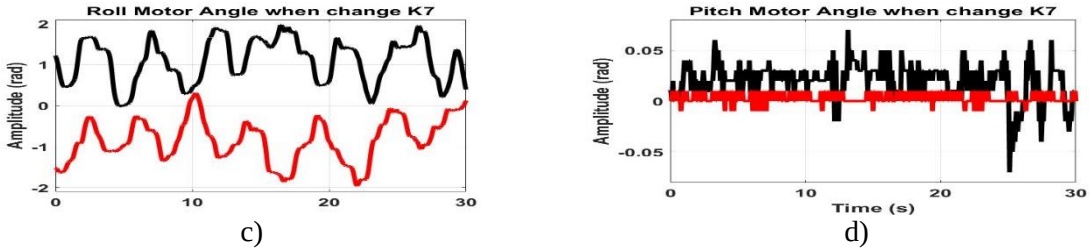

c) d)

Figure 11. *Modify Q_7 value of Roll axis b) Modify Q_7 value for Pitch axis c) Output result of the disk motor d) Output result of the wheel motor (Black line is K7=1; Red line is K7=0.3)*

Comment:

When increasing Q_7, figures 11 a-b show that roll angle oscillates significantly around 0.3 rad, and pitch angle oscillates around -0.5 rad. Figures 11 c-d indicate the roll motor oscillates slightly around 1 rad, meanwhile, the pitch motor oscillates steadily around -0.5 rad with an amplitude of about 0.5 rad.

When decreasing Q_7, figures 11 a-b prove the roll and pitch angles oscillate around 0.25 rad, but the pitch angle oscillates with a smaller amplitude compared to the roll angle. Figures 11 c-d prove the roll motor oscillates slightly around -1 rad. Meanwhile, the pitch motor oscillates steadily around the equilibrium position with a relatively small amplitude.

4.9. Modify Q_8 value

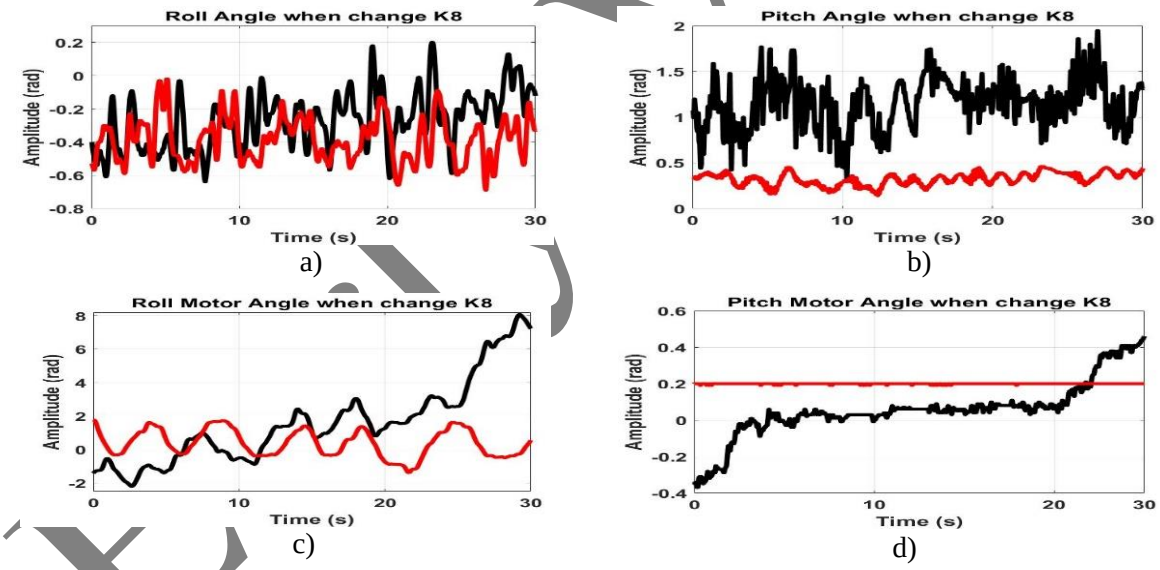

a) b) c) d)

Figure 12. *Modify Q_8 value of Roll axis b) Modify Q_8 value for Pitch axis c) Output result of the disk motor d) Output result of the wheel motor (Black line is K8=0.4; Red line is K8=0.05)*

Comment:

When increasing Q_8, figures 12 a-b show that the roll angle oscillates significantly and tends to gradually increase at -0.3 rad, while the pitch angle oscillates quite frequently around 1 rad. Figures 12 c-d illustrate the roll motor's oscillation gradually increases from -1.5 rad to 5 rad, meanwhile, the pitch motor starts from -0.35 rad, gradually reaches the equilibrium position at the 3rd second, and stabilizes. However, from the 20s, the signal tends to increase gradually to 0.4 rad.

When decreasing Q_8, figures 12 a-b prove the roll and pitch angles oscillate around -0.4 rad and 0.4 rad, but the pitch angle oscillates with a smaller amplitude compared to the roll angle. Figures 12 c-d indicate the roll motor oscillates slightly around 1 rad, meanwhile, the pitch motor oscillates steadily around 0.2 rad with a very small amplitude.

4.10. Video clip demonstration

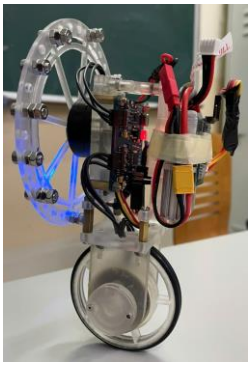

Figure 13. *Capture of a video animation of the unicycle robot. Source: The actual footage of the unicycle robot's operation process. https://www.youtube.com/shorts/lWePB0Ivu6o*

A snapshot of the unicycle robot's operation is presented in Figure 13. The image captures a moment from a 50-second video demonstration, which showcases the effectiveness of the LQR control scheme in managing the stability and movement of the one-wheel mobile robot. The video provides visual evidence that the LQR control strategy successfully maintains the robot's balance and navigational capabilities, despite the inherent instability of the unicycle design.

Regarding the mechanical structure of the unicycle robot is designed and 3D-printed using high-quality Clear Resin V5 (Form 4), known for its exceptional clarity, accuracy, transparency, and strong mechanical properties. 3D printing process can be found at Formlabs.

A snapshot of unicycle 's operation is presented in Figure 13. The image captures a moment from a 50-second video demonstration, which showcases the effectiveness of the LQR control scheme in managing the stability and movement of the one-wheel mobile robot. Video provides visual evidence that LQR control strategy successfully maintains robot's balance and navigational capabilities, despite the inherent instability of the unicycle design.

5. Conclusions

This paper has contributed a new type of balancing robot in Vietnam, providing a mathematical model of a Unicycle Robot analyzed from two basic models: the inverted pendulum model and the reaction wheel balance inverse pendulum model. The LQR controller is applied to the Unicycle Robot by designing two parallel LQR controllers to control the Robot's Pitch and Roll axes, allowing the examination of the controller and resulting in various behaviors when the Q are changed. Thereby, it helped us succeed in hardware design, developing the controller, and controlling the new type of balancing robot.

However, there are still some limitations, as the Robot does not yet have a controller for the Yaw axis, leading to the inability to control the Robot's forward/backward movement and direction. Additionally, the behavior of the Robot under changing loads has not been examined.

Acknowledgement

This paper is part of a project for Ho Chi Minh City University of Technology and Education (HCMUTE) students of the year 2025, funded by HCMUTE. We, the authors, are grateful for this support.

Conflict of Interest

The authors declare no conflict of interest.

REFERENCES

[1] A. Schoonwinkel, "Design and test of a computer stabilized unicycle," *Ph.D. dissertation*, Stanford Univ., Stanford, CA, 1987. Retrieved from: http://bicycle.tudelft.nl/schwab/Bicycle/BicycleHistoryReview/Schoonwinkel1987.pdf

[2] Z. Sheng and K. Yamafuji, *"*Postural stability of a human riding a unicycle and its emulation by a robot,*" IEEE Trans. Robot. Autom.*, vol. 13, no. 5, pp. 709–720, 1997, doi: 10.1109/70.631232.

[3] J. H. Lee *et al.*, "Novel air blowing control for balancing a unicycle robot," *in Proc. IEEE/RSJ Int. Conf. Intell. Robots Syst.*, pp. 2529–2530, 2010, doi: 10.1109/IROS.2010.5649120.
[4] J. Lee *et al.*, "Decoupled Dynamic Control for Pitch and Roll Axes of the Unicycle Robot," *IEEE Transactions on Industrial Electronics*, vol. 60, no. 9, 2013, doi: 10.1109/TIE.2012.2208431.
[5] S. I. Han and J. M. Lee, "Balancing and Velocity Control of a Unicycle Robot Based on the Dynamic Model," *IEEE Transactions on Industrial Electronics* 62, pp. 405-413, 2015, doi: 10.1109/TIE.2014.2327562.
[6] J. Shen and D. Hong, "OmBURo: A Novel Unicycle Robot with Active Omnidirectional Wheel," *IEEE International Conference on Robotics and Automation (ICRA)*, pp. 8237-8243, 2020, doi: 10.1109/ICRA40945.2020.9196927.
[7] NXTway-GS (self-balancing two-wheeled robot) controllerdesign, LEGOMindstorm, Enfield, CT, Tech.Rep [Online]. Available: http://www.mathworks.com/matlabcentral/fileexchange/19147.
[8] R. C. Dorf and R. H. Bishop, Modern Control System, 10th Edition: Optimal Control System. Upper Saddle River, NJ: Pearson, 2005.
[9] Y. Tanaka and T. Murakami, "A Study on Straight-Line Tracking and Posture Control in Electric Bicycle," *IEEE Trans. Ind. Electron.*, vol. 56, no. 1, pp. 159–168, 2009, doi: 10.1109/TIE.2008.927406.
[10] D. H. Vu *et al.*, "A Survey of Linear Control for Unicycle Robot," *Robotica & Management*, vol. 29, no. 1, pp. 45-54, 2024, doi: 10.24193/rm.2024.1.8

Thi Ai Van Nguyen (Student ID: 20151108). She is a student of the Faculty of High-Quality Training, Ho Chi Minh City University of Technology and Education (HCMUTE). She is interested in researching nonlinear control and intelligent control for systems.
Email: 20151108@student.hcmute.edu.vn. ORCID: https://orcid.org/0009-0004-0337-147X

Dinh Hau Vu (Student ID: 20151362). He is a student of the Faculty of High-Quality Training, Ho Chi Minh City University of Technology and Education (HCMUTE). He is interested in researching nonlinear control and intelligent control for systems.
Email: 20151362@student.hcmute.edu.vn. ORCID: https://orcid.org/0009-0009-2609-618X

Van Thuyen Ngo currently works at University of Technology and Education Ho Chi Minh as Chairman of the board. He received the Ph.D. degree in automation and control engineering from University of Technology Sydney (UTS), Australia in 2008. He was recognized as an Associate Professor by the State Council for Professorship in 2018. His research interests are fuzzy systems, intelligent control, observer and controller design for uncertain system, automation in industrial, SCADA.
Email: thuyen.ngo@hcmute.edu.vn, thuyennv@hcmute.edu.vn. ORCID: https://orcid.org/0009-0006-2605-7787

Tran Minh Nguyet Nguyen received B.S. degree in electrical-electronics engineering from Ho Chi Minh City University of Technology and Education, Ho Chi Minh City, Vietnam, in 2024 and M.S. degree in control and automation engineering from Ho Chi Minh City University of Technology, Ho Chi Minh City, Vietnam, in 2009. She is currently a lecturer with Department of Automatic Control, Ho Chi Minh City University of Technology and Education (HCMUTE), Vietnam. She is also the member of the Dynamics and Robotic Control (DRC) laboratory. Her research interests include intelligent control, nonlinear control and robotics.
Email: nguyetntm@hcmute.edu.vn. ORCID: https://orcid.org/0009-0002-8707-3036

Vi Do Tran received the Master degree in Electrical Engineering from the HCM University of Technology and Education, Vietnam, in 2015. He received the PhD in Bio Robotics at the Bio Robotics Institute, Scuola Superiore Sant'Anna in Pisa, Italy in 2018. His research interests are in the fields of rehabilitation robotics, assistive technologies and human-robot interaction From December 2018 until now, he has worked as a lecturer at the HCM University of Technology and Education, Vietnam.
Email: dotv@hcmnute.edu.vn. ORCID: https://orcid.org/0000-0001-9836-8118

Dinh Phu Nguyen He was born in Vietnam in 1972. He graduated from Ho Chi Minh City University of Technology and Education with a B.S degree in Electrical and Electronics Engineering in 1995 and a M.S degree in Electronic and Communication from Ho Chi Minh City Polytechnic University, in 2003. Since 1995, he has been a lecturer in the Faculty of Electrical and Electronics at Ho Chi Minh City University of Technology and Education. His research interests include the design of microcontroller practice kits, digital practice kits, microcontroller application controllers and FPGA chips. He has written teaching books on microprocessors, practical books on microcontrollers, and practicing digital IC design using VHDL.
Email address: phund@hcmute.edu.vn. ORCID: https://orcid.org/0009-0001-4761-4777

Van Dong Hai Nguyen currently works at the Faculty of Electrical and Electronic, University of Technology and Education Ho Chi Minh. He received the B.S. degree in automation and control engineering from Ho Chi Minh University of Technology, Vietnam in 2009; the M.S. degree in automation and control engineering from Ho Chi Minh University of Technology, Vietnam in 2011, and the Ph.D. degree in automation and control engineering from University of Craiova, Rumani in 2018. Since 2012, he has been a lecturer at Ho Chi Minh City University of Education and Technology, Vietnam. His research interests are fuzzy systems, intelligent control, observer and controller design for uncertain system.
Email: hainvd@hcmute.edu.vn. ORCID: https://orcid.org/0000-0001-7726-5128

Minh Tai Vo is currently a lecturer at the Faculty of Electronic Engineering 2, Posts and Telecommunications Institute of Technology, Ho Chi Minh City, Vietnam. He previously served as a senior technical officer at RMIT University Vietnam and as an automation engineer at Intel Products Vietnam, with tenures of 1.5 years and 3 years, respectively. He earned his BEng degree in Automation and Control Engineering Technology from Ho Chi Minh University of Technology and Education (HCMUTE) in 2020 and an MSc degree in Control Engineering and Automation from Ho Chi Minh City University of Technology (HCMUT), VNU-HCM, in 2024. His research interests focus on control engineering.
Email: taivm@ptit.edu.vn. ORCID: https://orcid.org/0000-0002-5463-2500

Binh Hau Nguyen currently works as a lecturer at the Electronics Department 2 of the Posts and Telecommunications Institute. He received his Master's degree in Control and Automation from the Ho Chi Minh City University of Technology in 2018. His research interests include industrial robotics, SCADA systems, system balancing, and control of systems such as the inverted pendulum and industrial robots.
Email: haunb@ptit.edu.vn. ORCID: https://orcid.org/0009-0009-7231-0343

JTE HCMUTE
ISSN: 2615-9740
JOURNAL OF TECHNICAL EDUCATION SCIENCE
Ho Chi Minh City University of Technology and Education
Website: https://jte.edu.vn
Email: jte@hcmute.edu.vn

Minh Tam Nguyen was born in Ben Tre province, Vietnam. He received the Ph.D. degree in Engineering Science from the University of Technology, Sydney, Australia in 2010. His research interests include system modeling, intelligent and robust control, soft-computing, and power system control.
Email: tamnm@hcmute.edu.vn. ORCID: https://orcid.org/0009-0000-8230-1373